Composite Structures 204 (2018) 301–312

Contents lists available at ScienceDirect

Composite Structures

journal homepage: www.elsevier.com/locate/compstruct

Nonlinear in-plane instability of functionally graded multilayer graphene reinforced composite shallow arches

Zhicheng Yang[a], Jie Yang[b,*], Airong Liu[a], Jiyang Fu[a]

[a] Guangzhou University-Tamkang University Joint Research, Centre for Engineering Structure Disaster Prevention and Control, Guangzhou University, Guangzhou, China
[b] School of Engineering, RMIT University, PO Box 71, Bundoora, VIC 3083, Australia

ARTICLE INFO

Keywords:
Buckling
Postbuckling
Graphene nanoplatelets
Functionally graded nanocomposite
Analytical solutions

ABSTRACT

This paper investigates the in-plane instability of functionally graded multilayer composite shallow arches reinforced with a low content of graphene platelets (GPLs) under a central point load. The GPL weight fraction, which is a constant within each individual GPL reinforced composite (GPLRC) layer, follows a layer-wise variation along the thickness direction. The effective Young' modulus of the GPLRC is estimated by modified Halpin-Tsai micromechanics model. The virtual work principle is used to establish the nonlinear equilibrium equations for the FG-GPLRC arch fixed or pinned at both ends which are then solved analytically. A parametric study is conducted to examine the effects of distribution pattern, weight fraction, and size of GPL nanofillers and the geometrical parameters of the FG-GPLRC arch on its buckling and postbuckling behaviors. The conditions for multiple limit point buckling to occur in an FG-GPLRC pinned arch are also discussed. It is found that GPL nanofillers have a remarkable reinforcing effect on buckling and postbuckling performances of nanocomposite shallow arches.

1. Introduction

Graphene, a two-dimensional monolayer of carbon atoms, and its derivatives such as graphene nanoplatelets (GPLs) have become an emerging area of extensive research efforts in advanced composite materials (ACM) [1–3]. It has been experimentally demonstrated that GPL nanofillers greatly outperform other reinforcement materials such as glass fibres, carbon fibres, and carbon nanotubes (CNTs) to achieve polymer or metal based nanocomposites with significantly improved stiffness and strength [3–5]. Rafiee et al. [6,7] measured and compared the mechanical properties of epoxy nanocomposites reinforced by GPLs and CNTs respectively and found that both GPLs and CNTs have significant reinforcing effects on the Young' modulus, tensile strength and fracture toughness compared with the pure epoxy but the performance of GPLs is much better than that of CNTs. Liu et al. [8,9] investigated the mechanical properties of alumina ceramic composites reinforced by GPLs and indicated that the flexural strength of the composite is considerably higher than that of monolithic ceramic samples. Tang et al. [10] showed the experimental results that the graphene/epoxy nanocomposites with highly dispersed graphene have higher strength and fracture toughness.

Functionally graded materials (FGMs) are characterized by a continuous and smooth change in both composition profile and material properties along one or more than one directions to achieve desired structural performance [11–14]. By combining the advantages of both GPLs and FGMs, Yang and his co-workers [15] proposed a multilayer functionally graded GPL reinforced composites (FG-GPLRC) in which the weight fraction of GPLs follows a layer-wise variation along the thickness direction and showed that the buckling and postbuckling resistance of such an FG-GPLRC beam can be remarkably improved, compared with its counterpart with uniformly distributed GPLs. Wu et al. [16] studied the dynamic instability of functionally graded multilayer graphene nanocomposite beams in thermal environment and found that adding a very small amount of GPLs into polymer matrix with more GPLs dispersed near the top and bottom surfaces can effectively increase the natural frequency and reduce the size of the unstable region. Similar results were also observed in the linear and nonlinear structural behaviors of FG-GPLRC beams and plate structures under various loading conditions [17–21].

Arch is a widely used important structure or structural element in aerospace, civil and marine engineering sectors [22–24]. Pi and Bradford preformed a series studies on the stability and buckling behavior of homogeneous arches [25–31]. Liu et al. [32] experimentally and analytically investigated the in-plane dynamic instability of arches owing to parametric resonance. Hodges [33] presented a non-linear theory for stretching and in-plane bending of isotropic beams with constant initial

* Corresponding author.
E-mail address: j.yang@rmit.edu.au (J. Yang).

https://doi.org/10.1016/j.compstruct.2018.07.072
Received 31 May 2018; Received in revised form 5 July 2018; Accepted 16 July 2018
Available online 27 July 2018

Nomenclature

A_{11}, B_{11}, D_{11}	stiffness components
b	width of the FG-GPLRC arch
B_0	$=B_{11}/A_{11}h$
E	effective Young's modulus
E_{GPL}, E_m	Young's modulus of the GPL and matrix
H(θ)	step function
h	total thickness of the FG-GPLRC arch
h_L	thickness of GPLRC layers
N	axial compressive force
N_F	critical axial force for FG-GPLRC fixed arches
N_P	critical axial force for FG-GPLRC pinned arches
N_L	total number of the layers
M	bending moment
P	dimensionless static load
R	radius of the FG-GPLRC arch
r_{11}	$=\sqrt{\kappa/A_{11}}/h$
S	arc length
V^*_{GPL}	total volume fraction of GPLs
$\widetilde{v}$	dimensionless radial displacement
W	total virtual potential energy
W_{GPL}	GPL weight fraction
$\widetilde{w}$	dimensionless axial displacement
δW	the variation of the total potential energy
2Θ	central angle
ρ_{GPL},ρ_m	mass densities of GPLs and the polymer matrix
ξ_L,ξ_T	GPL nanofillers geometry factors
a_{GPL}, b_{GPL}, t_{GPL}	length, width and thickness of GPLs
ε_m, ε_b	membrane strain, bending strain
$\delta_D(\theta)$	dirac-delta function
μ	dimensionless axial force parameter
κ	effective bending stiffness
β	dimensionless axial force parameter
β_b	critical dimensionless axial force parameter for bifurcation buckling
λ	dimensionless geometrical parameter of the FG-GPLRC arch
λ_b	critical geometric parameters for bifurcation buckling

curvature lying in their plane of symmetry. Moghaddasie and Stanciulescu [34] obtained the exact displacement field, load-bearing capacity and the locus of critical points for a pinned elastic half-sine shallow arch under static loading in a thermal environment. In spite of its practical importance, studies on functionally graded arches are still limited. Bateni and Eslami [35,36] and Asgari et al. [37] investigated the stability phenomenon of FGM shallow arch under a uniform radial pressure, a central concentrated force and a thermal load, respectively and discussed the influences of material property gradient, geometrical characteristics, and boundary conditions on the stability behavior of the FG circular shallow arches. To the best of authors' knowledge, no previous work has been done on the buckling and postbuckling of functionally graded graphene reinforced nanocomposite arches.

This paper aims to fill in this gap and investigate the buckling and postbuckling behaviors of functionally graded multilayer GPLRC arches under a central point load. The effective Young' modulus of GPLRCs is estimated by modified Halpin-Tsai micromechanics based model. Virtual work principle is used to establish both nonlinear equilibrium equations and buckling equilibrium equations for FG-GPLRC arches either fixed or pinned at both ends which are solved analytically. A parametric study is carried out to explore the effects of the distribution pattern, weight fraction, and size of GPL nanofillers and geometrical parameters of the arch on the buckling and postbuckling performance of FG-GPLRC arches. The system parameters that are capable of producing better reinforcing effect are identified.

2. Materials model of FG-GPLRC arch

Fig. 1a shows a shallow FG-GPLRC arch with a central angle 2Θ, arc length S, radius of curvature R, total thickness h and cross section $b \times h$ that is composed of multiple GPLRC layers of the same thickness h_L. It is assumed that each individual GPLRC layer is made from a mixture of an isotropic polymer matrix and GPLs that are uniformly dispersed and randomly oriented hence can be considered to be isotropic homogeneous. Along the thickness direction, however, GPL weight fraction follows a layer-wise variation. Two through-thickness functionally graded GPL distribution patterns (X-GPLRC and O-GPLRC) together with the uniform GPL distribution pattern (U-GPLRC) as a special case are considered in the present study. As can be seen from Fig. 1b, both top and bottom layers are GPL rich in X-GPLRC while this is reversed in O-GPLRC, and the GPL content is the same throughout the thickness in U-GPLRC.

Without the loss of generality, the FG-GPLRC arch with an even number of layers is considered. The GPL volume fraction of the kth layer for different GPL distributions is defined as [15–20]

$$\text{U - GPLRC:} \quad V^k_{GPL} = V^*_{GPL} \tag{1}$$

$$\text{X - GPLRC:} \quad V^k_{GPL} = 2V^*_{GPL}\,|2k-N_L-1|/N_L \tag{2}$$

$$\text{O - GPLRC:} \quad V^k_{GPL} = 2V^*_{GPL}(1-|2k-N_L-1|/N_L) \tag{3}$$

where N_L is the total number of individual layers. The total volume fraction of GPLs can be calculated from its weight fraction W_{GPL} as

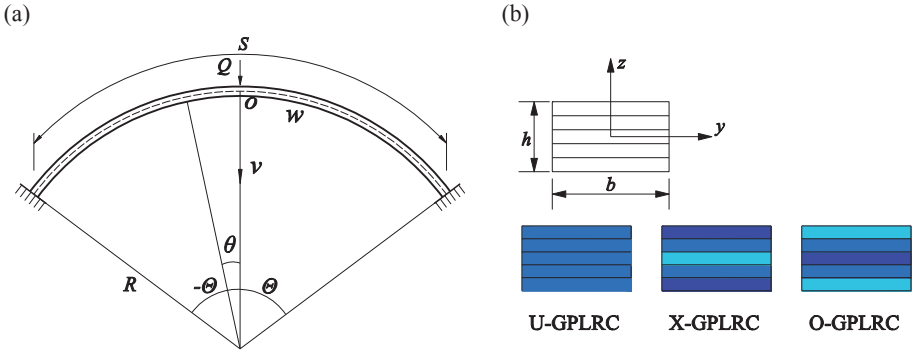

Fig. 1. Configuration and coordinate system of an FG-GPLRC arch.